

## ORIGINAL ARTICLE

# Design of an Expression System for Rapid Production of Tri-Functional Antibody Substitution of Hybridoma Technology

Mohammad Reza Dehghani<sup>1</sup>, Reza Ahangari Cohan<sup>2</sup>, Kobra Omidfar<sup>3</sup>, Mohammad Hossein Ghahremani<sup>4,5</sup>

<sup>1</sup> Department of Molecular Medicine, School of Advanced Technologies in Medicine, Iran University of Medical Sciences, Tehran, Iran

<sup>2</sup> Department of Pilot Nanobiotechnology, New Technologies Research Group, Pasteur Institute of Iran, Tehran, Iran

<sup>3</sup> Biosensor Research Center, Endocrinology and Metabolism Research Institute, Tehran University of Medical Sciences, Tehran, Iran

<sup>4</sup> Department of Molecular Medicine, School of Advanced Technologies in Medicine, Tehran University of Medical Sciences, Tehran, Iran

<sup>5</sup> Department of Pharmacology-Toxicology, School of Pharmacy, Tehran University of Medical Sciences, Tehran, Iran

Received: 23 Feb. 2017; Accepted: 02 Jul. 2017

**Abstract-** Tri-functional antibodies, as an effective novel tumor targeting agents, are composed of anti-CD3 rat IgG2b and an anti-tumor antigen antibody. We have intended to develop a novel drug system to induce the apoptosis of HER2-expressing tumor cells, activate and engage cytotoxic T lymphocytes, natural killer cells, and macrophages. In addition, the drug can inhibit programmed death ligand 1 (PDL-1)-expressing tumor cells. We have designed a mammalian vector system suitable to express the trifunctional antibody composed of antiHER2×human-CD80: human-IgG1Fc antibody. This antibody contains four chains of anti-HER2/CL, anti-HER2/CH<sub>1-3</sub>, B7.1/CL, and B7.1/CH<sub>1-3</sub> within the human IgG1 framework and so the vector system will simultaneously express the four chains. The amino acid/nucleotide sequences datasets were retrieved from the GenBank, UniProtKB and PDB databases. The heavy and light chains variable domain framework regions and complementarity determining regions of scA21 antibody were determined by IMGT/V-QUEST and Paratome software. The amino acid sequences of tri-functional antibody chains manually were assembled and converted to DNA sequences by sequence manipulation suite software. The adapting codon usage of these DNA sequences was performed by JCAT software. Finally, the secondary structures of obtained RNAs from the DNAs were individually analyzed by RNAfold program. The Prodigy equilibrium dissociation constant, a ratio of  $k_{off}/k_{on}$ , between the antibody and its antigen for hantiHER2VHCH-HER2, hantiHER2VLCL-HER2, CD80CH-CD28, and CD80CL-CD28 were equal to 3.60E-10, 3.10E-9, 1.10E-8 and 2.70E-10; respectively. These findings were confirmed the composition and nano-molar affinity of the respective constructs. A single specific no-cloning expression vector, pHuChTriomAb, was designed *in silico* with a desirable length of 8.292 Kbps and bidirectional expression potential for the four chimeric antibody chains. This construct was designed, and gene codon usage adapted to be expressed within CHO cells and secreted a trifunctional antibody into the cell culture medium by interleukin 21 signal peptide. This robust expression system for rapid production of tri-functional antibody has been designed to substitute hybridoma technology (quadroma and trioma) with the facilitated purification of the trifunctional antibody from the antibody variants.

© 2018 Tehran University of Medical Sciences. All rights reserved.

*Acta Med Iran* 2018;56(3):140-150.

**Keywords:** Insilico; Tri-functional antibody; Cancer; Immunotherapy; Biotechnology

## Introduction

Cancer is a complicated disease with many different types of assorted clinical therapeutics. Advances in cancer treatment are important in the detection of suitable targets for therapy. Developing targeted receptor tyrosine kinases is one of the most effective approaches for cancer treatment. These receptors play a

significant role in the progression to aggressive tumor growth and poor prognosis. The human epidermal growth factor receptor (HER) family includes EGFR (HER 1 or ErbB-1), HER2/c-neu (ErbB-2), HER3 (ErbB-3), and HER4 (ErbB-4) high-affinity receptor tyrosine kinases (1,2). HER2 over-expression is involved in tumor proliferation, division, and angiogenesis, indicating neoplastic progression (3,4).

**Corresponding Author:** M.H. Ghahremani

Department of Pharmacology-Toxicology, School of Pharmacy, Tehran University of Medical Sciences, Tehran, Iran  
Tel: +98 21 66959102, Fax: +98 21 66959102, E-mail address: mhghahremani@tums.ac.ir

Some cancers such as breast, pancreatic, gastric, ovarian, and cholangiocarcinoma over-express the HER2 receptor. Thus, this receptor has been targeted for the eradication of tumor cells. ChA21 is an antibody to HER2; it binds to the extracellular subdomain-I of HER2 and efficiently induces apoptosis in ovarian carcinoma cells (SK-OV-3 cells).

Tri-functional antibodies (TriomAb), which are effective-novel tumor targeting agents, are composed of anti-CD3 rat IgG2b and an anti-tumor antigen antibody. Drugs such as catumaxomab and ertumaxomab are effective at low doses, show higher efficacy than monoclonal antibodies, and have been shown to be effective in clinical phase III and II trials (5). Ertumaxomab targets HER2/neu, CD3, and FcγRI/III receptors to assemble a tri-cell complex in the tumor, T, and accessory cells. The anti-tumor efficacy of ertumaxomab against HER2/neu low-tumors which are resistant to Herceptin has been demonstrated previously (5). Similarly, Catumaxomab targets T-cell CD3, EpCAM tumor antigen, and accessory cells FcγRI/III receptors and resembles ertumaxomab; however, it targets different tumor cells. Catumaxomab has been examined in phase III clinical trials (5).

The B7.1 or CD80 costimulatory ligand is a member of the cell surface immunoglobulin superfamily and is expressed on the surface of antigen-presenting cells, including activated B cells, macrophages, and dendritic cells. Its dimers interact with T-cell CD28 and CTLA-4 receptors in two separate pathways. The CD80/CD28 pathway induces T-cell activation, cytokine production (i.e., IL-1, IL-2, IL-6, IL-12, TNF-α, IFN-γ), and cytotoxic T-lymphocyte (CTL) generation. The CD80/CTLA-4 pathway induces T-cell tolerance and immune response regulation. The CD80-Fc fusion protein may dramatically affect the proliferation and cytotoxicity of normal lymphocytes (6). In this regard, the tumor cells such as breast and ovarian cancers escape anti-tumor cellular immunity by expressing programmed death ligand-1 (PDL-1), which interacts with T-cell PD-1 to

result in T-cell apoptosis. It contributes to tumor cell rescue from Fas ligand-mediated lysis, which may maintain tumor cells *in situ* (7).

Although it has been proved that the triomabs are potent and effective therapeutic agents in cancer therapy, the design and production of these complex structures have been difficult. Since the function of triomabs depends on expression of the IgG chains for specific sites to target and initiate the cell death, design of a plasmid with proper cassettes is essential in antibody production. In this study, we have designed a single specific no-cloning expression vector *in silico*, pHuChTriomAb, for the TriomAb, antiHER2×human-B7.1:human-IgG1Fc antibody, which contains four chains of anti-HER2/CL, anti-HER2/CH<sub>1-3</sub>, B7.1/CL, and B7.1/CH<sub>1-3</sub> within the human IgG1 framework. This antibody can induce the apoptosis of HER2-expressing tumor cells and activated cytotoxic T cells, natural killer cells, and macrophages as well as inhibiting the PDL-1-expressing tumor cells.

## Materials and Methods

### GenBank, UniProtKB, and PDB databases

The antibody experimental data sets of A4.6.1 (anti-VEGF-A) scFv, Hu2.10 scFv (humanized anti-VEGF), and Hu2.0 scFv were used. The data sets of cha21 antiHER2 (3H3B), scA21 antiHER2 (2GJJ), human B7.1 (1I8L), Newcastle disease virus (NDV) furin-cleavage (PIZA05N277, human IgG1 framework (1HZH-H&K), foot-mouth disease virus (FMDV) 2A peptide (P03305), EF1-HTLV promoter (KC176267), CMV-HTLV promoter (KC176268), EM2KC promoter (AB902850), SV40-βglobin polyA (JO2400), Zeocin resistance sh-ble gene (EDN63766), ColE1 (JO1566), and pUC57 replication origin (γ14857) amino acid and nucleotide sequences were obtained from the GenBank, UniprotKB and PDB databases (Table 1, Suppl. Table 1).

**Table 1. Retrieving affinity data of antibody-antigen and receptor-ligand**

| Antibody/Receptor       | Antigen/Ligand | kD(nM) |
|-------------------------|----------------|--------|
| <b>A4.6.1scFv</b>       | VEGF-A         | 1.6    |
| <b>scA21scFv</b>        | ErbB2          | 13.1   |
| <b>Human B7.1(CD80)</b> | CD28           | 400    |
| <b>CTLA-4</b>           | CD28           | 400    |

The affinity of some antibody scFv forms and ligand to VEGF-A antigen and CD28 receptor has been represented, respectively. These affinities contributed us to compare them with bioinformatics outputs

### IMGT/V-QUEST (ImMunoGeneTics)

IMGT/V QUEST is an integrated system used for the standardized analysis of immunoglobulin (IG) rearranged nucleotide sequences. IMGT/V QUEST identifies frameworks (FRs) and complementarity determining regions (CDRs) of IG variable domains (8). Murine scA21 VH & VL and murine A4.6.1 VH & VL nucleotide sequences in FASTA format files were input into the IMGT/V-QUEST portal.

### Paratome

The Paratome web server predicts the antigen-binding regions (ABRs) of an antibody (Ab), given amino-acid sequences, or 3D structures corresponding to input file type, FASTA, or pdb. It exploits the consensus region dataset derived from the structural alignment of a non-redundant set of all known antibody-antigen complexes. The web server identifies the submitted antibody sequence or structure, which corresponds to the consensus ABRs. The paratome web server is available at [http://www.ofranlab.org/paratome/\(9\)](http://www.ofranlab.org/paratome/(9)). Murine scA21 VH & VL (anti-HER2) and murine A4.6.1 (anti-VEGF) VH & VL amino acid sequence datasets (10, 11) in FASTA format were input into the paratome portal.

### Chimeric and humanized dataset

The required datasets for designing the chimeric protein framework consisted of a signal peptide (interleukin-21 signal peptide, IL-21 SP), HuscA21 VHCH, Newcastle disease virus furin cleavage site, foot-mouth disease virus 2A peptide, HuscA21 VLCL, B7.1CH, and B7.1CL.

### SMS (Sequence manipulation suite): Reverse Translate

SMS Reverse Translate accepts a protein sequence as input and uses a codon usage table to generate a DNA sequence, by representing the most likely non-degenerate coding sequence. This program is available at [www.bioinformatics.org/sms2/rev-trans.html](http://www.bioinformatics.org/sms2/rev-trans.html). The two constructed chimeric protein frameworks above were converted to DNA frameworks using SMS: Reverse Translate. The input data sets were in FASTA format.

### FLAG and His tagging

Two different tags were used, including a 3×FLAG tag and a His-3×FLAG tag. These were individually considered for designing gene cassettes.

### JCAT (Java codon adaptation tool)

JCAT is an application for adapting target gene

codon usage to most sequenced prokaryotes and selected eukaryotic gene expression. It is used to improve heterologous protein production. This application does not require the manual definition of highly expressed genes (10). The JCAT output is graphics and as codon adaptation index (CAI) values given for both the pre-improved sequence and the improved sequence. JCAT is integrated into the PRODORIC database that hosts information for various organisms to fulfill the requested calculations. JCAT is accessible at <http://www.prodoric.de/JCAT>. The two obtained DNA frameworks were optimized using the JCAT tool based on codon bias of the considerable host cell (CHO cells).

### GeneScript rare codon analysis tool

The two optimized DNA frameworks were evaluated using the GeneScript rare codon analysis tool. It is accessible at [www.genscript.com/cgi-bin/tools/rare-codon-analysis](http://www.genscript.com/cgi-bin/tools/rare-codon-analysis).

### Sequence editor (DNA to RNA converter)

Sequence editor accepts a nucleic acid sequence in FASTA format (without name). It converts DNA sequences into RNA sequences in FASTA format. It is accessible at [www.fr33.net/seqedit.php](http://www.fr33.net/seqedit.php). The two confirmed optimized DNA frameworks were converted to RNA using sequence editor.

### RNAfold program (Vienna RNA package)

RNAfold is a program for predicting RNA secondary structure. The program uses only the default settings (11) and is available at <http://rna.tbi.univie.ac.at/cgi-bin/RNAfold.cgi>.

### TriomAb expression vector datasets

The required dataset including the CMV-HTLV promoter, two TriomAb gene cassettes, SV40 polyA, pUC57 ori, EF1-HTLV promoter, EM2CK promoter, and zeocin resistance gene (sh-ble gene) was applied to design a TriomAb expression vector (see Suppl. Table 1).

### SnapGene viewer

The TriomAb expression vector features were highlighted, and the orientations were determined using SnapGene Viewer. The TriomAb expression vector was plotted using SnapGene viewer.

## Results

### FRs and CDRs discrimination

The first step in manipulating FR regions of antibody

VH and VL is discriminating FRs and CDRs within the VH and VL amino acid sequences. Hence, we applied the IMGT-gap tool for discrimination. The system analyzed the sequences and displayed CDR and FR boundaries (see Suppl. Tables 2,3).

#### ABRs determination

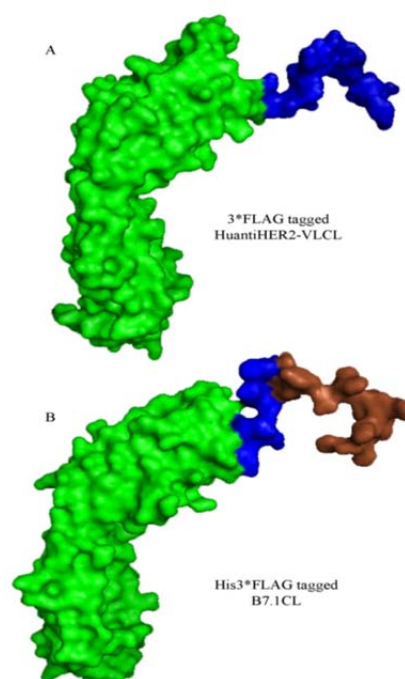
The presence of the amino acid residues of ABRs for binding to the antigen is necessary. Therefore, the ABRs within the VH and VL amino acid sequences of scA21 and A4.6.1 were predicted utilizing the Paratome tool. This was conducted to identify which amino acids must be restrained and which must be manipulated (see Suppl. Table 4).

#### Multiple alignments and humanizing antibody

In order to humanize the murine antiHER2VH and VL structures, it was required to retrieve the prevalent sequences of the VH and VL structures from humans. The VH-III and VL-I regions, are the most prevalent human antibody variable regions whose sequences were retrieved from the UniProtKB database. Next, these amino acid residue sequences with similar sequences to the murine antiHER2 VH and VL were aligned using the PRALINE multiple alignment web server. Two types of humanization were utilized; one based on bevacizumab human VH&VL-FRs and the other based on the prevalent VH-III&VL-I FRs. The exchangeable regions (FRs) determined in the initial section of the study were determined using the IMGT and Paratome servers. Bevacizumab human VH-FR1 (EVQLVESGGGLVQPGGSLRLSCAASG), VH-FR2 (WIRQAPGKGLE), VH-FR3 (AADFKRRFTISLDTSASTVYLQMNSLRAEDTAVY YCA), VH-FR4 (WGQGTLLTVSS), VL-FR1 (DIQMTQSPSSLSASVGDRTITCSAS), VL-FR2 (WYQQKPGKAPK), VL-FR3 (VPSRFSGSGSGTDYTLTISSLQPEDFATYYC), and VL-FR4 (TFGQGTKVEIK) were utilized for humanizing the constructs. Humanization of HuantiHER2scFvN2 was performed using the prevalent sequences of human VH-FRs and VL-FRs, including VH-FR1 (EVQLVESGGDLVKPGESLRLSCKAS), VH-FR2 (WVRKNTGKGLE), VH-FR3 (NQKFKNRFTISRDDSKNTLYLQLNSLTSEDVAVY YC), VH-FR4 (WGQGTTVTVSS), VL-FR1 (DIQMTQSPSSLSVSVGDRTITCRAS), VL-FR2 (WYQQKPGQAPK), VL-FR3 (GVPSRFSGSGSGTDFTLTISLQPEDVATYYC), and VL-FR4 (TFGQGTKLEIKR).

#### Inserting FLAG and His tags within gene cassettes

An efficient method for purifying proteins is to utilize the peptide tags such as His tags. The purification tags of 3×FLAG (DYKDHDGDYKDHDIDYKDDDDK) and 9His3×FLAG (HHHHHHHHHDYKDHDGDYKDHDIDYKDDDDK) were inserted at the N-terminus of antiHER2VLCL and B71.CL; respectively (Figure 1). The individual 3×FLAG tag was utilized for the antiHER2CHCHVLCL gene cassette. The chimeric 9His-3×FLAG tag was utilized for the B7.1CHB7.1CL gene cassette. The tag peptide sequences were converted to nucleotide sequences according to the codon usage of CHO cells for gene cassettes.



**Figure 1.** Tag locations. A: Blue region within the N-terminus of the HuantiHER2-VLCL model illustrates the 3×FLAG tag. B: Blue and brown regions within the N-terminus of the B7.1CL model illustrate the 3×FLAG and 9His tags; respectively. These models confirmed that the tags were exposed and detectable by relevant antibodies

#### Conversion of protein primary structure to nucleotide primary structure

The expression vector design of the primary structure of protein chains must be converted to primary nucleotide structures. This process was performed according to using standard codons in the SMS server.

#### Optimization of gene cassettes

It is necessary to optimize the expressing gene

cassettes according to the host cell, CHO cells, based on its codon usage to increase the probability of mRNA translation.

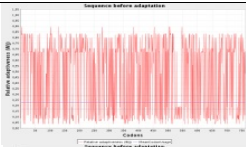
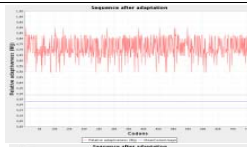
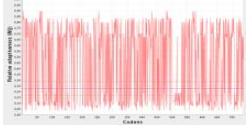
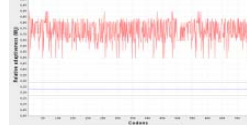
The criteria values of the CAI and GC-content for HuantiHER2 VHCH-VLCL and B7.1CH-B7.1CL gene cassettes before optimization were 0.30–56.27 and 0.26–53.2, respectively. The values of CAI and GC-content after optimization using the JCAT server were 0.71–64.92 and 0.72–63.46; respectively. The value range of CAI is from 0.0 to 1.00. Greater CAI values near 1.00 lead to more frequent codon usage in the considered sequence (Table 2).

### Evaluation of the optimized gene cassettes

The optimized primary nucleotide structures were evaluated using the gene evaluation software in the GeneScript server to determine the quality of the structure. The relevant software assessed the

improvement in the quality of HuantiHER2VHCH-VLCL and B7.1CH-B7.1CL optimized gene cassettes by determining CAI, GC-content, and codon frequency distribution (CFD) criteria according to codon usage in the species *Cricetulus griseus*. The CAI value of ideal and good levels of the expressed sequence is equal to 1.00 and more than 0.8, respectively. The percentage range of ideal GC-content is between 30% and 70%. Each peak out of the range negatively affects transcription and translation efficacy. The most frequent amino acid codon usage in a cassette-expressing organism has a CFD equal to 100%. In this study, the calculated values of CAI, GC-content, and CFD criteria for the HuantiHER2VHCH and B7.1CH-B7.1CL gene cassettes were 1.00, 63.51, and 100%, respectively (see Suppl. Table 5). Consequently, the quality of the gene cassettes for expressed in CHO cells according to codon usage bias of the host cell was confirmed.

**Table 2. DNA improvement**

|                             | Before adaptation |            |   | After adaptation |            |   |
|-----------------------------|-------------------|------------|---|------------------|------------|---|
|                             | CAI-Value         | GC-Content | Curve   | CAI-Value        | GC-Content | Curve   |
| <b>HuAntiHER2 VHCH-VLCL</b> | 0.3037            | 56.269     |   | 0.7137           | 64.919     |   |
| <b>HuB7.1CH-B7.1CL</b>      | 0.2872            | 53.207     |  | 0.7211           | 63.459     |  |

The DNAs of HuantiHER2 VHCH-VLCL and B7.1CH-B7.1CL gene cassettes based on codon usage of *Cricetulus griseus* for CHO host cell were optimized for silico. The relevant outputs have been shown as CAI and GC-content. These optimized findings showed the desirable states. CAI: Codon Adaptation Index

### Conversion of DNAs to mRNAs and evaluation of secondary structure

The primary structure of the gene cassettes was converted into RNA sequences, and the secondary structure of the RNAs was evaluated using RNA fold server. The ribosome binding site must be free to increase the expression potential in the host cell. The secondary structure analysis of HuantiHER2VHCH-VLCL mRNA and B7.1CH-B7.1CL mRNA using RNAfold represented the minimum free energy (MFE), frequency of MFE, ensemble diversity, and base pair probability in the ribosome binding site were (-94.3.63 Kcal/mol, 0.00%, 642.23, and 0.0) and (-886.94 Kcal/mol, 0.00%, 530.35, and 0.0), respectively. Most of the base pairs belonged to the mfe structure; however, these base pairs were in positions after 400 and after

800, suggesting that the structures did not slow the codon translation process, particularly when the ribosome binding sites were free. The initial regions of the structures contained blue and near blue color spectrum, suggesting that the base pair probability in the regions was very low. The very low base-pair probabilities in the regions confirmed that the sections of the mRNAs were free for ribosome binding. The large negative MFEs were created by two long mRNA sequences. The resulting mountain plots showed three curves, confirming the above probabilities (Table 3).

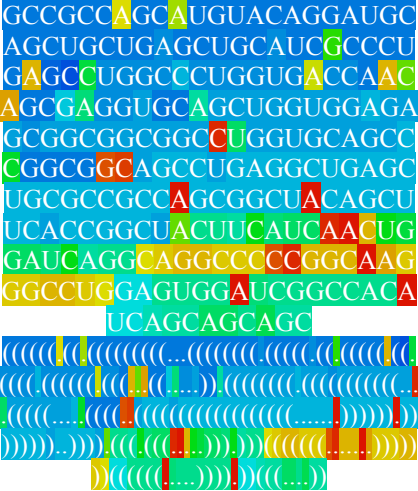

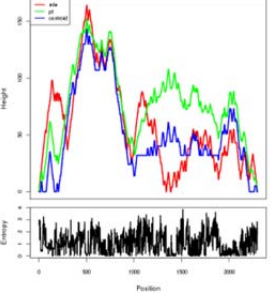


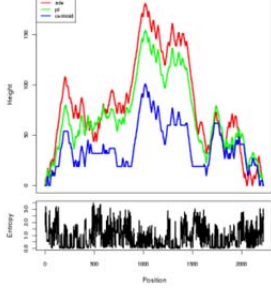
### Designing and plotting of pHuchiTriomAb

The composition of the HuantiHER2VHCH-VLCL gene cassette consisted of the hEF1 $\alpha$ - HTLV promoter, the relevant gene, and SV40 polyadenylation (pAn).

The B7.1CH-B7.1CL gene cassette consisted of the reverse complement CMV-HTLV promoter, the reverse complement of the relevant gene, and sv40pAn. The reverse complement EM2KC promoter was considered to be the sh-ble gene. This expression vector consisted of four parts; part 1: HuanTiHER2VHCH-VLCL, gene cassette, expressing antiHER2 heavy and light chains; part 2: B7.1CH—B7.1CL gene cassette, expressing CD28 inducer integrated to human IgG1 heavy and light chains; part 3: on pUC57, creating the potential for plasmid

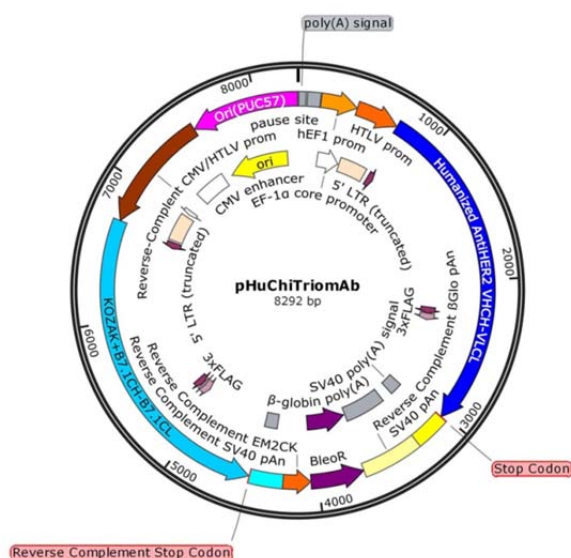
amplification in the bacterial cell; part 4: sh-ble gene cassette, creating the potential for zeocin resistance both in bacterial and eukaryotic cells. The pHuChiTriomAb expression vector was composed of 8292 base pairs; a length of less than 10,000 base pairs prevents breakage in the structure. The vector was designed to express bidirectional antibody chains. Each gene cassette was designed to express two heavy and light chains of the relevant antibody. SnapGene defines and determines the relevant features within the FASTA nucleotide sequence by plotting the vector (Figure 2).

**Table 3. Thermodynamic ensemble prediction**

| RNAs                                  | The optimal secondary structure in Dot-bracket notation                             | MFE secondary structure   | MFE(kcal/mol)/Frequency of MFE (%) | Base-pairing probability at ribosome binding Site | Mountain Plot   |
|---------------------------------------|---|---|------------------------------------|---|---|
| KOZAK-HuanTi-HER2CH-HuanTi-HER2CL RNA |   |   | -912.60/0.00                       | Very Weak   |   |
| KOZAK-B7.1CH-B7.1CL RNA               |  |  | -886.94/0.00                       | Very Weak   |  |

The mRNAs of optimized HuanTiHER2 VHCH-VLCL and B7.1CH-B7.1CL gene-cassettes were evaluated by RNAfold web server. It has been shown that the base-pairing probability at ribosome binding site is very weak





**Figure 2.** HuChiTriomAb expression vector. The no-cloning specific expression vector with a length less than 10 kbp and bidirectional expression potential for humanized antiHER2×human-B7.1: human-IgG1Fc tri-functional antibody with 94.3% human composition *in silico* was designed and then plotted using SnapGene software

## Discussion

As novel therapeutics, tri-functional antibodies are of growing interest because they can be used to support and explore new mechanisms of actions for disease treatments. The tri-functional antibodies are of particular interest due to their resemblance to conventional hIgG1 therapeutics. However, obtaining pure tri-functional antibody is challenging because of the complexities that arise from the co-expression of 2 pairs of heavy and light chains. Therefore, both designs of an effective therapeutic tri-functional antibody and an expression system contribute to the development of therapeutic antibody and efficient production methods. Here, for eliminating the problems of hybrid hybridoma technologies, we have been achieved to design an expression vector system without the need to cloning and completely specific for CHO host cell expressions. To confirm the success of engineering solutions, use of protein modeling, protein-protein docking and underestimating of antibody binding affinity to its antigen is critical.

Tri-functional antibodies, which are effective novel tumor targeting agents, are composed of anti-CD3 rat IgG2b and anti-tumor antigen antibody. The first studies of tri-functional antibodies highlighted two major limitations including the difficulty of producing large, homogeneous batches, and the lack of efficacy of murine antibody fragments. Human anti-mouse

antibody (HAMA) responses were seen in most treated patients, which severely decreased the efficacy of the murine molecules and excluded the possibility of multiple administrations.

Thus, we have designed a novel drug based on antibodies to induce the apoptosis of HER2-expressing tumor cells, activate cytotoxic T-cells, natural killer cells, and macrophages and inhibition of programmed death ligand 1 (PDL-1)-expressing tumor cells.

Our design is a TriomAb containing the humanized antiHER2×human-B7.1: human-IgG1Fc tri-functional antibody with 94.3% human composition *in silico*.

Based on benchmarking from the composition of the antibodies VH-III and VL-I, which are the most prevalent isoforms in the human body, substitution of human FR for murine FRs within the antiHER2scA21 antibody VH and VL was performed. This generated humanized (65%; 83/126) VH domain and 71% (81/114), which lacked a significant difference between the murine and humanized structures versus H, indicating a significant difference. The z criterion for humanized murine VH was determined as follows.

$$1. \quad Z = \frac{\frac{x_1}{n_1} - \frac{x_2}{n_2}}{\sqrt{p(1-p)(\frac{1}{n_1} + \frac{1}{n_2})}} \quad (1)$$

and

$$2. \quad p = \frac{x_1 + x_2}{n_1 + n_2}$$

and the results were 11.1, which was greater than  $z_{0.975} = 1.96(z_1 = \alpha/2, \alpha = 0.05)$ . Therefore, the  $H_0$  hypothesis was rejected; however, the  $H_1$  hypothesis was accepted. Hence, there was a significant difference between the humanized and murine antiHER2VH structures.

The  $z$  criterion for the humanized murine VL structure was 11.8, which is greater than  $z_{0.975} = 1.96$  ( $z_{1-\alpha/2}$ ,  $\alpha = 0.05$ ). Thus, the  $H_0$  hypothesis was rejected while the  $H_1$  hypothesis was accepted. There was a significant difference between the humanized and murine antiHER2 VL structures.

Prior to production, the quality of model structures should be calculated, and the interactions between protein-protein complexes should be analyzed based on rating scores for the efficient selection of structures. In addition, the protein models for integrating protein structures and building a single chimeric structure should be evaluated. This has been confirmed to determine the functional potential of protein structures not only in the chimeric state but also in the non-chimeric state.

Different scoring schemes were used for the output values and for the experimental study values. The different scores for structural different features indicated direct and similar relationships in accordance with experimental outputs and confirmed that the effectiveness of this drug design route and its evaluation in efficiency and usability.

This study contributes to the design TriomAbs and chimeric structures. In addition, there was overlap between the expected and observed results. Predicting the enhancement, reduction, and neutrality of chimeric structures from native functional or inducible structures and their affinities should be determined independently. This drug was designed to be exploited against cancer cells, HER2- and PDL-1-expressing cancer cells, such as breast and ovarian cancers. The Prodigy equilibrium dissociation constant, a ratio of  $k_{off}/k_{on}$ , between the antibody and its antigen ( $P-K_D$ ) for hantiHER2VHCH-HER2, hantiHER2VLCL-HER2, CD80CH-CD28, and CD80CL-CD28 were equal to  $3.60E-10$ ,  $3.10E-9$ ,  $1.10E-8$  and  $2.70E-10$ ; respectively. These findings were confirmed the composition and nano-molar binding affinity of the respective models.

pHuchiTriomAb expression system possesses two robust eukaryotic promoters, hEF1 $\alpha$ - HTLV and CMV-HTLV promoters, was designed to express two antibody mRNAs, including HuantiHER2VHCH<sub>1-3</sub>-HuantHER2VLCL and B7.1CH<sub>1-3</sub>-B7.1CL. Utilizing the contrived autocleavage-2A-peptide between HuantiHER2VHCH<sub>1-3</sub> and HuantiHER2VLCL; and B7.1CH<sub>1-3</sub> and B7.1CL antibody constructs contributed to the separation of the HuantiHER2VHCH<sub>1-3</sub> and HuantiHER2VLCL, and B7.1CH<sub>1-3</sub> and B7.1CL antibody construct from each other. The chains were assembled and secreted from CHO cells using the interleukin 21signal peptide. Also the purification tags of 3 $\times$ FLAG and 9His3 $\times$ FLAG which inserted at the N-terminus of antiHER2VLCL and B7.1CL; respectively, would contribute to two steps purification (Figure 1). At the first step, the variants of could be purified which possess 3 $\times$ FLAG at the N-terminus of antiHER2VLCL. At the second step, the variants of could be purified which possess both 3 $\times$ FLAG at the N-terminus of antiHER2VLCL and 9His3 $\times$ FLAG at the N-terminus of B7.1CL. The individual 3 $\times$ FLAG tag was utilized for the antiHER2CHCHVLCL gene cassette. The attached tags are cleavable by enterokinase enzyme. This expression system was designed to eliminate the need for hybrid hybridoma (quadroma and trioma) technologies.

In this study, four applications were successfully utilized. First, prediction of the antibody-antigen and

ligand-receptor complex binding affinity in native and chimeric forms were determined by evaluating  $P-K_D$  based on the experimental and *in silico* data. Second, a humanizing TriomAb with 94.3% human composition *in silico* was developed. Third, a desirable single specific no-cloning expression vector, pHuchiTriomAb, with a desirable length that of less than 10 Kbp and bidirectional expression potential for four different chimeric antibody chains was designed. This vector was designed to be expressed within CHO cells and secrete the antibody into the cell culture medium. Moreover, the vector contained two suitable tags for protein purification. Fourth, the design, modeling, binding potential estimation, and engineering of a TriomAb, HuantiHER2 $\times$ human-B7.1: human-IgG1Fc antibody, which contained four chains of anti-HER2/CL, anti-HER2/CH<sub>1-3</sub>, B7.1/CL, B7.1/CH<sub>1-3</sub> within the human IgG1 framework were evaluated. This study is an *in silico* model of vector to produce a triomab with equal production of antibodies to induce apoptosis in HER2-expressing tumor cells as well as engaging cytotoxic T-cells, natural killer cells, and macrophages in PDL-1-expressing tumor cells.

## Acknowledgements

This research team included researchers from the Iran University of Medical Sciences, Tehran University of Medical Sciences, and Pasteur Institute of Iran organizations. These organizations are gratefully acknowledged. The research is financially supported by Deputy of Research, Tehran University of Medical Science Grant No. 91-04-87-20423 to MHG.

## References

1. Scott A, Wolchok J, Old L. Antibody therapy of cancer. *Nat Rev Cancer* 2012;12:278-87.
2. Cho H, Mason K, Ramyar K, Stanley A, Gabelli S, Denney D, et al. Structure of the extracellular region of HER2 alone and in complex with the Herceptin Fab. *Nature* 2003;421:756-60.
3. Troise F, Monti M, Merlino A, Cozzolino F, Fedele C, Russo Krauss I, et al. A novel ErbB2 epitope targeted by human antitumor immunoagents. *FEBS J* 2011;278:1156-66.
4. Piccart-Gebhart M, Procter M, Leyland-Jones B, Goldhirsch A, Untch M, Smith I, et al. Trastuzumab after Adjuvant Chemotherapy in HER2-Positive Breast Cancer. *New England J Med* 2005;353:1659-72.
5. Chelius D, Ruf P, Gruber P, Ploscher M, Liedtke R,



## Tri-functional antibody expression system

- Gansberger E, et al. Structural and functional characterization of the trifunctional antibody catumaxomab. *MAbs* 2010;2:309-19.
6. Peach R, Bajorath J, Naemura J, Leytze G, Greene J, Aruffo A, et al. Both Extracellular Immunoglobulin-like Domains of CD80 Contain Residues Critical for Binding T Cell Surface Receptors CTLA-4 and CD28. *J Biol Chem* 1995;270:21181-7.
  7. Homicsko K, Coukos G. Targeting Programmed Cell Death 1 in Ovarian Cancer. *J Clin Oncol* 2015;33:3987-9.
  8. Brochet X, Lefranc M, Giudicelli V. IMGT/V-QUEST: the highly customized and integrated system for IG and TR standardized V-J and V-D-J sequence analysis. *Nucleic Acids Res* 2008;36:W503-8.
  9. Kunik V, Ashkenazi S, Ofra Y. Paratome: an online tool for systematic identification of antigen-binding regions in antibodies based on sequence or structure. *Nucleic Acids Res* 2012;40:W521-4.
  10. Grote A, Hiller K, Scheer M, Munch R, Nortemann B, Hempel D et al. JCat: a novel tool to adapt codon usage of a target gene to its potential expression host. *Nucleic Acids Res* 2005;33:W526-31.
  11. Hofacker I. Vienna RNA secondary structure server. *Nucleic Acids Res* 2003;31:3429-31.

**Supplementary Table 1. Retrieving and Confirming Dataset. The obtained sequences from NCBI and UniProtKB were analyzed by using BLAST. This analysis confirmed the relevant sequence alignment.**

| Max Score | Total Score | Query cover (%) | E-Value | Identity (%) | Accession  | Entry                                   | UniprotKB | PDB ID  |
|-----------|-------------|-----------------|---------|--------------|------------|---|-----------|---------|
| 946       | 946         | 100             | 0.0     | 100          | 1 HZH-H    | IgG1                                    | Po1857    | 1 HZH-H |
| 946       | 946         | 100             | 0.0     | 100          | 1 HZH-K    | IgG1                                    | Po1834    | 1 HZH-K |
| 522       | 522         | 100             | 0.0     | 100          | 3H3B-D     | Cha21                                   | -         | 3H3B    |
| 539       | 539         | 100             | 0.0     | 100          | 2GJJ       | Sca21                                   | -         | 2GJJ    |
| 602       | 602         | 100             | 0.0     | 100          | 118L-B     | B7.1                                    | P33681    | 118L-B  |
| 4875      | 4875        | 100             | 0.0     | 100          | P03305     | FMDV-2Apeptide                          | P03305    | -       |
| 11049     | 11049       | 100             | 0.0     | 100          | Kc176267   | EF1-HTLV Promoter                       | -         | -       |
| 12022     | 12022       | 100             | 0.0     | 100          | Kc176268   | CMV-HTLV Promoter                       | -         | -       |
| 13900     | 14032       | 100             | 0.0     | 100          | AB902850   | EM2KC                                   | -         | -       |
| 9683      | 9951        | 100             | 0.0     | 100          | Jo2400     | SV40-Bglobin polyA                      | -         | -       |
| 503       | 503         | 100             | 8e-179  | 100          | 2WHU-D     | KRFP                                    | Q1JV70    | 2WHU-D  |
| 496       | 496         | 100             | 4e-176  | 100          | P42212     | GFP                                     | P42212    | 1BFP    |
| 212       | 212         | 100             | 2e-68   | 100          | EDN63766   | Zeocin Resistance Gene                  | A6ZNA1    | -       |
| 264       | 264         | 100             | 3e-88   | 100          | P0C2PO     | Blasticidin-S Resistance Gene deaminase | POC2Po    | 1NN57   |
| 12273     | 12273       | 100             | 0.0     | 100          | JO1566     | CoLE1                                   | -         | -       |
| 5005      | 5005        | 100             | 0.0     | 100          | Y14837     | PUC57 Replication Origin                | -         | -       |
| 691       | 691         | 100             | 0.0     | 100          | PIZA05N277 | NDV                                     | -         | -       |

**Supplementary Table 2. VL-region IMGT analysis (ImMunoGeneTics). Annotation by IMGT/Automat (ImMunoGeneTics): After submitting nucleotide sequences of anti-HER2 Ab VL-region using IMGT tool, the data were analyzed, and the FRs& CDRs of the VL-region were identified.**

| Label             | Location/Qualifiers   |
|-------------------|---|
| <b>V-J-REGION</b> | IVLTQTPSSLPVSVGEKVTMTCKSSQTLTLYSNNQKNYLAWYQQKPGQSPKLLISWAFTRK<br>SGVPDRFTGSGSGTDFLTIGSVKAEDLAVYYCQQYSNYPWTFGGGTRLEIK<br>allele="Musmus IGKV8-30*01 F", gene="Musmus IGKV8-30" |
| <b>V-REGION</b>   | IVLTQTPSSLPVSVGEKVTMTCKSSQTLTLYSNNQKNYLAWYQQKPGQSPKLLISWAFTRK<br>SGVPDRFTGSGSGTDFLTIGSVKAEDLAVYYCQQYSN  |
| <b>FR1-IMGT</b>   | IVLTQTPSSLPVSVGEKVTMTCKSS   |
| <b>CDR1-IMGT</b>  | QTLTLYSNNQKNY   |
| <b>FR2-IMGT</b>   | LAWYQQKPGQSPKLLIS   |
| <b>CDR2-IMGT</b>  | AA_IMGT:WAF   |
| <b>FR3-IMGT</b>   | TRKSGVPDRFTGSGSGTDFLTIGSVKAEDLAVYYC   |
| <b>CDR3-IMGT</b>  | QQYSNYPWT   |
| <b>FR4-IMGT</b>   | FGGGTRLEIK  |

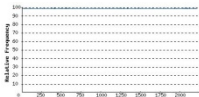
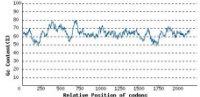
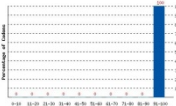
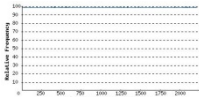
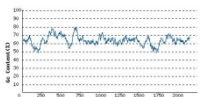
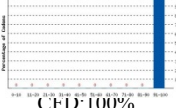
**Supplementary Table 3. VH-region IMGT analysis (ImMunoGeneTics). Annotation by IMGT/Automat: After submitting nucleotide sequences of anti-HER2 Ab VH-region using IMGT tool, the data were analyzed, and the FRs& CDRs of the VH-region were identified.**

| Label               | Location/Qualifier  |
|---------------------|---|
| <b>V-D-J-REGION</b> | QQSGPEVVKTGASVKISCKASGYSTGYFINWVKNSGKSPIEWIGHISSYATSTYNQKF<br>KNKAAFTVDTSSSTAFMQLNSLTSEDSAVYYCVRSGNYEEYAMDYWGQTSVTVS<br>allele="Musmus IGHV1-39*01 F", gene="Musmus IGHV1-39" |
| <b>V-REGION</b>     | QQSGPEVVKTGASVKISCKASGYSTGYFINWVKNSGKSPIEWIGHISSYATSTYNQKF<br>KNKAAFTVDTSSSTAFMQLNSLTSEDSAVYY   |
| <b>FR1-IMGT</b>     | QQSGPEVVKTGASVKISCKAS   |
| <b>CDR1-IMGT</b>    | GYSFTGYF  |
| <b>FR2-IMGT</b>     | INWVKNSGKSPIEWIGH   |
| <b>CDR2-IMGT</b>    | ISSYATS   |
| <b>FR3-IMGT</b>     | TYNQKFKNKAAFTVDTSSSTAFMQLNSLTSEDSAVYYC  |
| <b>CDR3-IMGT</b>    | VRSGNYEEYAMDY   |
| <b>FR4-IMGT</b>     | WGQTSVTVS   |

**Supplementary Table 4. Paratome Analysis. The Ag-binding sites (ABRs) of antiHER2 Ab VL & VH regions were identified using Paratome tool**

| ABR1  | ABR2          | ABR3          |
|---|---------------|---------------|
| QTLYSNNQKNYLA   | LLISWAFTRKS   | QQYSNYPW      |
| >paratome_2_Anti_HER2_VH_CHs (heavy chain)<br>QQSGPEVVKTGASVKISCKASGYSFTGYFINWVKKNSGKSPEWIGHISSYATSTYNQKFKNKAFTVDTSSSTAFMQLNSLTSEDS<br>AVYYCVRSGNYEEYAMDYWGQGTSTVTSASTKGPSVFPLAPSSKSTSGGTAALGCLVKDYFPEPVTVSWNSGALTSGVHTFPAVL<br>QSSGLYSLSSVVTVPSSSLGTQTYICNVNHKPSNTKVDKRVEPKSCDKTHTCPPCPAPELLGGPSVFLFPPKPKDTLMISRTPEVTCVV<br>VDVSHEDPEVKFNWYVDGVEVHNAKTKPREEQYNSTYRVVSVLTVLHQDWLNGKEYKCKVSNKALPAPIEKTKAKAGQPREPQ<br>VYTLPPSREEMTKNQVSLTCLVKGFYPSDIAVEWESNGQPENNYKTPPVLDSDGSFFLYSKLTVDKSRWQQGNVFCSCVMHEALH<br>NHYTQKSLSLSPGK |               |               |
| ABR1  | ABR2          | ABR3          |
| YSFTGYFIN   | WIGHISSYATSTY | VRSGNYEEYAMDY |

**Supplementary Table 5. Improved DNA Quality Evaluation. The DNAs of optimizedHuantiHER2 VHCH-VLCL and B7.1CH-B7.1CL gene cassettes were evaluated by gene evaluation software of Genescript server. The output thereof as CAI, GC-content, and CFD were shown. It confirmed the desirable quality of DNA optimization**

| Gene Cassettes       | Codon Adaptation Index (CAI)  | GC Content Adjustment GC curve  | Codon Frequency Distribution(CFD)   |
|----------------------|---|---|---|
| HuAntiHER2 VHCH-VLCL | <br>CAI:1.00  | <br>Average GC content: 63.51  | <br>CFD:100%  |
|                      | <br>CAI:1.00 | <br>Average GC content: 63.51 | <br>CFD:100% |